The Bedisk and Beray Circumstellar Disk Codes

T. A. A. Sigut

The University of Western Ontario, London, Ontario, Canada; asigut@uwo.ca

Abstract.
The Bedisk and Beray radiative transfer codes can be used to compute synthetic spectra and images for stars surrounded by circumstellar disks. The operation and atomic data requirements of these codes are discussed, as well as applications to the classical Be stars.

1. Classical Be Stars and Related Objects

Circumstellar disks are ubiquitous; newly forming stars are surrounded by accretion disks that act to transport material to the star and angular momentum away. Such disks dissipate by the time these stars arrive on the core hydrogen-burning main sequence; however, some massive, main sequence stars, corresponding to spectral type B with masses between 3 and 25 $M_\odot$, will find themselves again surrounded by a circumstellar disk in the course of their main sequence evolution. About one fifth of all main sequence B stars show observational evidence for such disks (Zorec & Briot 1997), such as emission lines in their spectra, an excess of infrared radiation compared to isolated stars, and polarization of their light. Such stars are classified as "B emission-line" stars or Be stars. Extensive interferometric observations of Be stars in the solar neighbourhood confirm that the circumstellar material is in the form of a thin, equatorial disk in Keplerian rotation about the central star (Quirrenback et al. 1997).

The Be stars are the most rapidly-rotating stars on the main sequence, often with rotation periods of just a day or two. This rapid rotation is thought to be the key driver of the process that ejects gas from the stellar photosphere into a disk (Rivinius et al. 2013). Such out-flowing disks are usually referred to as *decretion* disks. Models of stellar evolution with rotation demonstrate that internal redistribution of angular momentum via rotational mixing can produce episodes of *critical rotation* in which the effective gravitational acceleration at the stellar equator vanishes (Granada et al. 2013). Although the detailed physics of the gas ejection remains unknown, the outward transport of angular momentum via a decretion disk is an efficient mechanism to help the central star rid itself of its excess angular momentum (Krtička et al. 2011). After ejection, the subsequent evolution of the disk is well described by hydrodynamical evolution governed by viscous torques (Rivinius et al. 2013).

Be stars range from those visible to the unaided eye (such as γ Cassiopeia) to those detected in nearby galaxies. Large fractions of Be stars occur in the Large and Small Magellanic Clouds (Martayan et al. 2007), likely due to the low metallicities in these galaxies. For this reason, the Be stars are excellent laboratories for studying both stellar evolution with rotation and the complex hydrodynamical processes occurring in circumstellar disks. In addition to these Be stars, often called *Classical* Be stars, there are several other populations of closely related stars: Herbig Ae/Be stars exhibit many of the properties ascribed to the Be stars, with the added presence of dust emission and association with newly forming B stars still surrounded by their accretion disks. At the other end of the evolutionary scale are the sgB[e] stars, which may be examples of disk ejection via critical rotation in post main sequence evolution (Granada et al. 2016).

To study all of these systems, it is important to have computational tools that can predict spectra, overall spectral energy distributions (SEDs), and interferometric phases and visibilities, preferably in a unified way, in order to test disk formation and evolution mechanisms. In this contribution, I will describe one such code suite, `Bedisk/Beray`, and give examples of its application.

2. `Bedisk`

The `Bedisk` code (Sigut & Jones 2007) requires as input a user-specified density structure for the disk, $\rho(R, Z)$, and the fundamental parameters of the central B star, including its photoionizing radiation field. Then `Bedisk` enforces radiative equilibrium to determine the gas temperature at each point in the disk. The main heating source of the disk gas is photoionization by UV photons from the central star. At each disk location, the radiative transfer equation is solved along rays directed back to the central star, with the star's photospheric spectrum taken as the "upwind" boundary condition on the transfer equation. The mean intensity at each disk location can then be used to compute the photoionization heating. Cooling processes include escaping radiation formed by recombination and collisionally-excited line radiation. Currently `Bedisk` includes atomic models for the nine most abundant elements, each over several ionization stages. As a by-product of the radiative equilibrium calculation, atomic level populations are obtained which can be used to construct the monochromatic opacity and emissivity for use in further radiative transfer solutions.

A commonly-used disk density structure assumes an axisymmetric disk in which the total gas density in the equatorial plane falls as a power-law with distance. The vertical structure of the disk can be determined by enforcing hydrostatic equilibrium with vertical component of the star's gravitational acceleration. If we assume for the purposes of the density model only that the temperature in the disk can be represented by some average temperature, $T_{\rm HE}$, and that the disk is geometric thin, we obtain

$$\rho(R, Z) = \rho_0 \left(\frac{R_*}{R}\right)^n \, e^{-\left(\frac{Z}{H}\right)^2} \; . \tag{1}$$

Here R is the radial distance in the equatorial plane, R_* is the stellar radius, and Z is the vertical height above or below the plane. The base density of the disk, ρ_0, and the radial power-law index, n, are free parameters. The disk scale height is given by $H = H_0(T_{\rm HE})\,[R/R_*]^{3/2}$. The "hydrostatic" disk temperature, $T_{\rm HE}$, is commonly taken to be 60% of the central star's effective temperature. However, `Bedisk` can also integrate the hydrostatic equilibrium equation at each disk location R in a manner consistent with the vertical temperature distribution, eliminating the assumption of a constant $T_{\rm HE}$ (Sigut et al. 2009). The simple scale height model with a constant $T_{\rm HE}$ produces a flared-disk with $H \propto R^{3/2}$. The more realistic treatment considerable alters this prediction, particularly near the star.

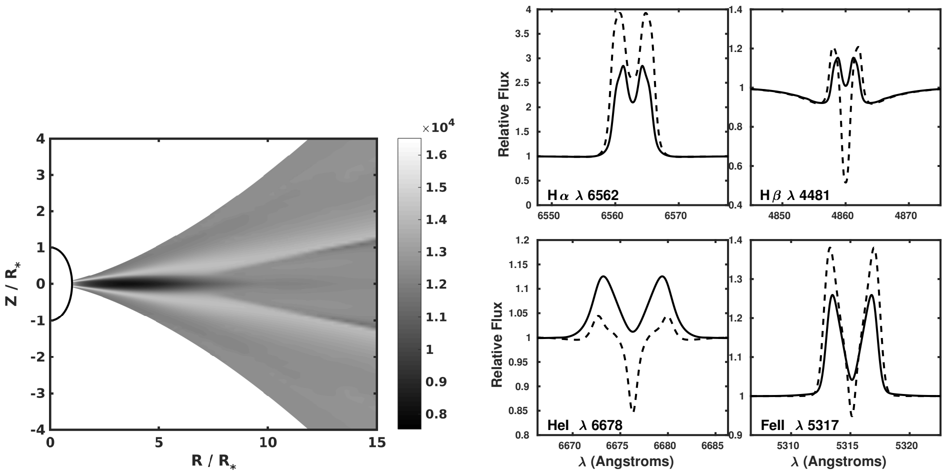

Figure 1. *Left*: The temperature distribution $T(R, Z)$ in a disk surrounding a B2V star computed with `Bedisk`. The colourbar indicates temperature in Kelvin. *Right*: Selected hydrogen, helium and iron emission lines produced by this disk as seen by a distant observer at two different inclination angles, $i = 65°$ (solid lines) and $i = 85°$ (dotted lines), computed by `Beray`. Note that for Hβ, the wings of the underlying photospheric absorption line are still visible.

Figure 1 shows $T(R, Z)$ for a disk with $\rho_0 = 7.5 \cdot 10^{-11}\,\mathrm{g\,cm^{-3}}$ and $n = 2.0$ surrounding a (assumed spherical) B2V star with $M = 9\,M_\odot$ and $R = 5\,R_\odot$. Note the very inhomogeneous temperature structure and the appearance of a inner, cool region near the star. At this location at UV frequencies, the optical depth along all rays back to the star are optically thick and the heating rate is reduced. Moving above (or below) this region reduces the optical depths for some rays and the temperature rises. Further away, the dense gas in the equatorial plane cannot shield the entire star and this cool zone disappears. Overall, the density-weighted average temperature in the disk is approximately 60% of the central star's T_{eff}; however, this does depend on the disk density parameters and the assumed chemical composition of the gas. Disks for Be stars in the Small Magellanic Cloud (SMC), for example, are hotter than this scaling relation due to the lower metallicities in the SMC (Ahmed & Sigut 2012).

An unrealistic aspect of Figure 1 is that the central star is spherical. The rapid rotation of Be stars distorts their shape and leads to the phenomena of gravitational darkening in which there is a temperature gradient with latitude across the stellar surface, with a hotter pole and cooler equator (Espinosa Lara & Rieutord 2011). This effect is implemented in both `Bedisk` and `Beray` (McGill et al. 2011, 2013) and must be included in any realistic analysis of Be star spectra (Ahmed & Sigut 2017).

2.1. Atomic Data Needs of `Bedisk`

In order to determine the microscopic rates of heating and cooling, the rate of each atomic process must be explicitly computed, and the required atomic level populations are found by enforcing statistical equilibrium. Included in these rate equations are both collisional processes that occur at the thermodynamic equilibrium rate set by the local temperature and density, and radiative processes that couple to the radiation field. Radiative processes typically do not occur at the thermodynamic rate as the radiation field is non-local due to photon loses from the boundaries and photon gains from other parts of the disk. This overall treatment is usually referred to as a "non-LTE" calculation, although thermodynamic equilibrium is recovered when non-local photons are unimportant. To compute the statistical equilibrium equations, all radiative bound-bound transitions require Einstein A_{ji} values and all bound-bound collision transitions require thermally-averaged collision strengths. Bound-free process require photoionization cross sections and collisional ionization rates. Heating and cooling must also include free-free processes (i.e. bremsstrahlung) but these do not enter into the rate equations. Of particular importance is photoionization as the ejected electrons are the principle source of heating. The rate of photoionization of level i of an atom or ion is given by

$$R_{i\kappa} = 4\pi \int_{\nu_0}^{\infty} J_\nu \, \sigma_{i\kappa}(\nu) \, \frac{d\nu}{h\nu} \; ; \tag{2}$$

therefore, accurate calculation requires a good estimate of both the mean intensity, J_ν, and the photoionization cross section. While the central star in Be systems are typically hot, $T_{\rm eff} > 10^4$ K, the disk gas can be considerable cooler, and photoionization of metals can make an important contribution to the gas heating. This implies that autoionizing resonances in $\sigma(\nu)$ can be important, although accurate resonant positions are not as important as overall strengths.

3. `Beray`

Of course, one does not directly observe gas density or temperature. The local thermodynamic conditions (T, ρ) must be used along with the atomic level populations to construct the gas opacity (χ_ν) and emissivity (η_ν) at each point in the disk. These can then be used in a formal solution of the radiative transfer equation along a series of rays directed at the observer to predict the specific intensity. This calculation is performed by the `Beray` code (Sigut 2011). The specific intensity from a patch of sky, $I_\nu(x,y)$, can be computed via

$$I_\nu = I_\nu^\circ \, e^{-T_\nu} + \int S_\nu \, e^{-\tau_\nu} d\tau_\nu \tag{3}$$

where the integral over optical depth τ_ν is along a straight ray passing through the system directed at the observer. I_ν° is the "upwind" boundary condition on the intensity, T_ν is the total optical depth along the ray, and S_ν is the monochromatic source function, defined as the ratio of the gas emissivity to opacity at frequency ν. For rays that originate on the stellar surface, I_ν° is fixed by the photospheric spectrum, otherwise $I_\nu^\circ = 0$. The fundamental quantity produced by `Beray` is the monochromatic intensity image of the star-disk system, $I_\nu(x,y)$, where x and y are Cartesian coordinates on the sky. Some Be stars are close enough to be resolved by interferometers, and in this case, the predicted interferometric visibilities and phases follow from the Fourier transform of $I_\nu(x,y)$. For more distant and unresolved objects, one can only measure the integrated intensity, or flux, as a function of frequency,

$$F_\nu = \int I_\nu(x,y) \, \frac{dx\,dy}{D^2} \; , \tag{4}$$

where the integral is over the image on the sky and D is the distance to the star. This equation can be used to compute both spectral line profiles for individual elements and overall SEDs.

The right panel of Figure 1 shows some example line profiles computed by Beray using the disk temperature/density model of the left panel. Using the level populations produced by Bedisk, Beray can compute profiles for transitions between any of the included energy levels. While Hα is the most commonly-modelled emission line in Be stars, many other elements also produce emission lines, including He I, Fe II, and Mg II. In the profiles shown in Figure 1, the underlying photospheric absorption line is consistently included. For rays that terminate on the stellar surface, an appropriately Doppler shifted (due to the star's rotation), non-LTE absorption line profile is used as the upwind boundary condition on the transfer equation. Doppler shifts along the ray due to the disk's rotation are included in the transfer equation in the observer's frame. Figure 1 also shows that the inclination of the system, the angle between the line of sight and the stellar rotation axis, has a strong controlling effect on the observed spectrum. Doubly-peaked emission lines are predicted for intermediate inclinations ($i = 65^\circ$ is shown), which become deep shell absorption for higher inclinations ($i = 85^\circ$ is shown). In a shell line, the line centre flux is reduced as the rays pass through the densest part of the disk. In Figure 1, this is particularly evident for Hβ.

4. Application to the Classical Be Stars

The Bedisk/Beray code suite has been used extensively to model the emission line spectra, spectral energy distributions (SEDs), and interferometric visibilities of Be stars. The focus of much of this work is on the modelling of Hα emission line profiles to determine the range of disk density parameters (ρ_0, n) appropriate to Be star disks (Silaj et al. 2010, 2014). The power law index n seems to be associated with the dynamical state of the disk (Vieira et al. 2017), either dissipating ($1.5<n<3$), steady, ($3 < n < 3.5$), or building ($n > 3.5$). In addition, ρ_0 and n can be used to estimate the disk mass if an estimate of the disk radius is available. Arcos et al. (2017) use the disk radius containing 90% of the Hα light to determine the Hα disk masses for a large sample of southern-sky Be stars. Sigut et al. (2015) and Jones et al. (2017) analyzed interferometric observations for the bright Be stars o Aqr (B7IVe) and 48 Per (B3Ve), which spatially resolve the disks, to determine disk masses (Figure 2, left panel). All of these results are compared by Arcos et al. (2017) to the predictions of critically-rotating stellar evolutionary models (Granada et al. 2013) computed under the assumption that disk eject acts to remove sufficient angular momentum from the star to prevent super-critical rotation. As shown in the right panel of Figure 2, the overall trend of disk mass with stellar mass is similar, but the disk masses (which are lower limits) generally lie above the predicted masses.

As Bedisk/Beray can model lines for elements other than hydrogen, precision abundance analysis of the central B stars of Be systems can be attempted. Here "corruption" of the photospheric spectrum by circumstellar emission and gravitational darkening is consistently modelled. Ahmed & Sigut (2017) searched for nitrogen over-abundances in a sample of Be stars from the MiMeS survey (Wade et al. 2014) as a diagnostic of rotational mixing. Nitrogen overabundances were found in about 1/3 of the sample, similar to results found for normal B stars. This is a slightly puzzling result as previous studies of normal B stars have focused on slow rotators. However, it is consistent with Dunstall et al. (2011), who found no difference in nitrogen abundance between the B and Be stars of the SMC.

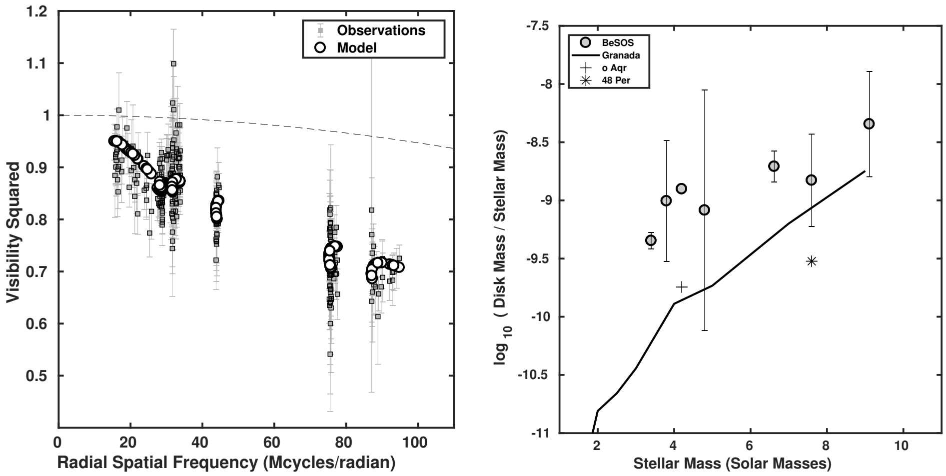

Figure 2. *Left*: Fit to the observed interferometric visibilities of the Be star 48 Per. The `Beray` model points are for $\rho_0 = 10^{-10}$ g cm^{-3}, $n = 3.0$, $i = 45°$ and $R_{\rm disk} = 50\,R_*$. The reduced χ^2 of the fit is 1.45. Adapted from Jones et al. (2017). *Right*: Comparison of the median Hα disk masses in the BeSOS sample of southern Be stars to the stellar evolution predictions of Granada et al. (2013). The error bars represent the 1σ dispersion in the observed disk masses. The individual Be stars 48 Per and o Aqr are as indicated. Adapted from Arcos et al. (2017).

Acknowledgments. I would like to thank the University of Western Ontario's Faculty of Science and Research Western for financial support.

References

Ahmed, A., & Sigut, T. A. A., 2017 MNRAS, 471, 3398
Ahmed, A., & Sigut, T. A. A., 2012 ApJ, 744, 191
Arcos, C., Jones, C. E., Sigut, T. A. A., Kannan, S., & Curé, M. 2017, ApJ 842, 48
Dunstall, P. R., Brott, I., Dufton, P. L., et al., 2011, A&A. 536, A65
Espinosa Lara, F., & Rieutord, M., 2011, A&A, 533, A43
Granada, A., Sigut, T. A. A., Jones, C. E., et al., 2017, ASP Conference Series Volume 508, 81
Granada, A., Ekström, S., Georgy, C. et al., 2013, A&A, 553, A25
Jones, C. E., Sigut, T. A. A., Grzenia, B. J., Tycner, C., & Zavala, R., 2017, ApJ, 843, 24
Krtička, J., Owocki, S. P., & Meynet, G., 2011, A&A, 527, A84
Martayan, C., Floquet, M., Hubert, A. M., et al., 2007, A&A, 472, 577
McGill, M. A., Sigut, T. A. A., & Jones, C. E., 2013, ApJS, 204, 2
McGill, M. A., Sigut, T. A. A., & Jones, C. E., 2011, ApJ, 743, 111
Quirrenback, A., Bjorkman, K. S., Bjorkman, J. E., et al., 1997, ApJ, 479, 477
Rivinius, T., Carciofi, A. C., & Martayan, C., 2013, A&ARv 21, 69
Sigut, T. A. A., Tycner, C., Jansen, B., & Zavala, R. T. 2015, ApJ, 814, 159
Sigut, T. A. A., 2011, ASP Conference Series 272, 426
Sigut, T. A. A., McGill, M. A., & Jones, C. E., 2009, ApJ, 699, 1973
Sigut, T. A. A., & Jones, C. E., 2007, ApJ, 668, 481
Silaj, J., Jones, C. E., Sigut, T. A. A., & Tycner, C., 2014, ApJ 795, 82
Silaj, J., Jones, C. E., Tycner, C., Sigut, T. A. A., & Smith, A. D., 2010, ApJS, 187, 228
Vieira, R. G., Carciofi, A. C., Bjorkman, J. E., et al., 2017, MNRAS, 464, 3071
Wade, G. A., Grunhut, J., Alecian, E., et al., 2014, IAU Symposium 302, 265
Zorec, J., & Briot, D., 1997, A&A, 1997, 318, 443